Electrical and Magnetic Properties of TiO and VO†

M. D. Banus,* T. B. Reed, and A. J. Strauss
Lincoln Laboratory, Massachusetts Institute of Technology, Lexington, Massachusetts 02173
(Received 23 July 1971)

The cubic compounds TiO_x and VO_x have a broad homogeneity range with x varying from about 0.75 to 1.30 and a total vacancy content varying between 11 and 20%. Golden TiO_x is a typical metal with a temperature- and composition-independent resistivity of about 3×10^{-3} Ω cm, a Seebeck coefficient varying from +1 to −10 μV/°C, a susceptibility of less than 10^{-4} emu/mole and a superconducting transition temperature between 0.4 and 1.0 K for all compositions. VO_x behaves in a qualitatively similar manner for $x<1.0$. However, it exhibits semiconductor behavior for $x>1.0$, where its resistivity is highly temperature and composition dependent with an activation energy ($150<T<300$ K) rising to about 4×10^{-2} eV for $x=1.3$. The Seebeck coefficient curve of VO_x is sigmoid, with α increasing from −12 to +22 μV/°C as x increases from 0.8 to 1.3. The magnetic susceptibility can be described by using a temperature-independent susceptibility and a Curie-Weiss term. VO_x is not a superconductor above 0.3 K for any composition. The total number of vacancies in these compounds can be reduced as much as 22% by annealing at 1300 °C at pressures of about 60 kbar. This decrease in vacancy concentration is accompanied by a decrease in resistivity and Seebeck coefficient. The superconducting transition temperature of TiO_x is increased to as high as 1.0 K. Although TiO_x samples as normally prepared by arc melting are cubic with random vacancies at low temperatures, related ordered structures can be produced by annealing certain compositions at atmospheric pressure. Annealing samples with $x=1.0$ below the transition temperature of 900 °C produces an ordered monoclinic structure whose properties are discussed.

I. INTRODUCTION

The relationships among chemical composition, structure, and other physical properties of solids can be effectively studied by the introduction of small changes in composition and/or structure. But most compounds, and even alloys, have discrete structures and compositions that can only be varied in large steps. The compounds TiO_x and VO_x are of particular interest because they have a very wide homogeneity range, extending over $0.75\leq x\leq 1.30$ for both compounds. The cation and anion vacancy concentrations change continuously over this range in an orderly fashion. Interest is further enhanced by the presence in each compound of partially filled, narrow d bands and by the possibility of removing vacancies from the structure by annealing at high pressure. For some compositions of TiO_x, annealing at atmospheric pressure creates closely related ordered structures of lower symmetry.

TiO_x and VO_x have been studied by numerous workers during the past twenty years, and a rather extensive bibliography summarizing this work has been presented in Ref. 1. (These compounds will subsequently be referred to generically as TiO and VO and more specifically as TiO_x and VO_x when it is necessary to specify exact compositions.) However, each investigator used his own methods of preparation and characterization so that it is dangerous to make inferences, for example, by comparing the Seebeck voltage measured by one investigator with the conductivity measured by another. This study includes data on the lattice parameter, density, vacancy concentration, resistivity, Seebeck coefficient, magnetic susceptibility, and superconducting transition temperature for well-characterized samples of each system, including a few single crystals, several vacancy-ordered samples, and specimens annealed at high pressure to reduce the vacancy concentration.

II. EXPERIMENTAL

About fifty ingots were prepared for each system, covering the entire homogeneity range. Single crystals with the approximate composition $x=1.29$ were grown by an arc-Czochralski technique; polycrystalline samples with the remaining compositions were prepared by arc melting and casting.[2] The cast samples, as prepared, showed very broad x-ray diffraction lines for some compositions. Therefore, most samples were annealed for 24–48 h at 1300–1500 °C in argon (TiO_x) or vacuum (VO_x), after which no broadening of the x-ray pattern could be detected. Samples were also prepared outside the homogeneity range to determine the limits of this range. All samples were examined metallographically, and only measurements on single-phase samples are reported here. Densities and lattice parameters were measured by the methods described in Ref. 1. The oxygen-to-metal ratio x in MO_x was determined by combustion to TiO_2 or V_2O_5 and calculated from

$$x=y-(g_2-g_1)(M+16y)/16g_2\ , \qquad (1)$$

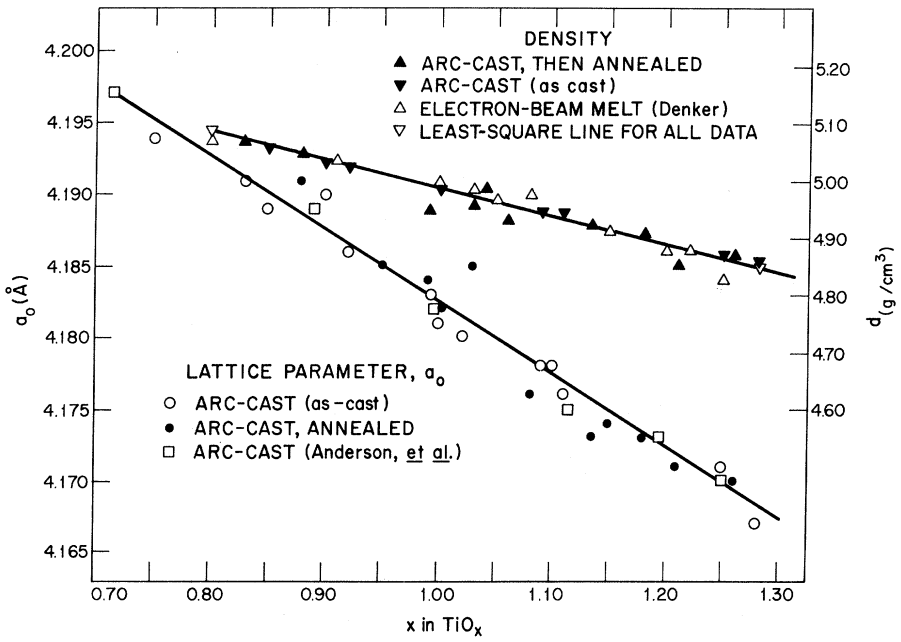

FIG. 1. Lattice parameter a_0 and measured density d of TiO_x as a function of x.

where y is the ratio of oxygen to metal atoms in the fully oxidized compound, g_1 and g_2 are the initial and final weights of the samples, and M is the atomic weight of the metal. The vacancy concentrations were calculated from

$$f_M = da_0^3 N/4(M+16), \quad f_O = xf_M \ , \tag{2}$$

where f_M and f_O are the fractions of vacant metal and oxygen sites, d is the measured density, a_0 is the lattice parameter, and N is Avogadro's number. The samples were analyzed with a spark-source mass spectrometer, which gave the following principal impurities:

TiO: Al-52, Si-110, Cr-54, total of all others < 35 ppm ,

VO: Ni-72, Fe-122, Ca-190, S-200, P-116, Si-400 , Al-200, Mg-80, total of all others < 40 ppm .

Microcombustion and micro-Kjeldahl tests showed that typically the TiO samples contained 250 ppm C and 90 ppm N, while the VO samples contained 100 ppm C and 130 ppm N.

Resistivities were measured by the dc van der Pauw technique, [3] using electrical contacts made with either spring-loaded point probes, indium applied by ultrasonic soldering, or silver-impregnated epoxy resin. Details of other electrical measurements will be found in previous papers. [4,5]

III. EXPERIMENTAL RESULTS

A. Cubic TiO

The lattice parameters a_0 and measured densities d of about twenty TiO samples are plotted as a function of x in Fig. 1. The vacancy concentrations, calculated from these data according to Eq. (2), are shown schematically in Fig. 2. The resistivities for various compositions as a function of $1/T$ are shown in Fig. 3 along with the activation energies taken in the interval $200 < T < 300$ K. The resistivities at 77 and 300 K are shown as a function of x in Fig. 4. It can be seen that the resistivity of cubic TiO_x is essentially independent of both temperature and composition, although an extremely small activation energy does increase slightly with x. On the other hand, the resistivity of the ordered monoclinic phase (formed by annealing cubic $TiO_{1.0}$ below the transition temperature) has a metallic temperature coefficient and is much lower than the resistivity of the cubic phase. [1,4] In earlier experiments, [1,5,6] the resistivity measured for cubic samples with x near 1.00 was intermediate between those of all the other compositions and that of the monoclinic phase, as shown in Fig. 7 of Ref. 1. However, it has been found that "splat" cooling or rapid gas quenching gives cubic samples with resistivities consistent with other TiO_x compositions, presumably because there is no incipient transition to the monoclinic phase.

The Seebeck coefficient of TiO_x varies as a function of composition (Fig. 5) from 1.4 μV/°C at $x = 0.78$ to -12 μV/°C at $x = 1.24$. This change in sign is consistent with the Hall coefficient data of Takeuchi and Suzuki, [6] who report $R_H = 2.7 \times 10^{-4}$ cm^3/C at $x = 0.82$ and $R_H = -0.8 \times 10^{-4}$ cm^3/C at $x = 1.23$. No magnetic susceptibility could be de-

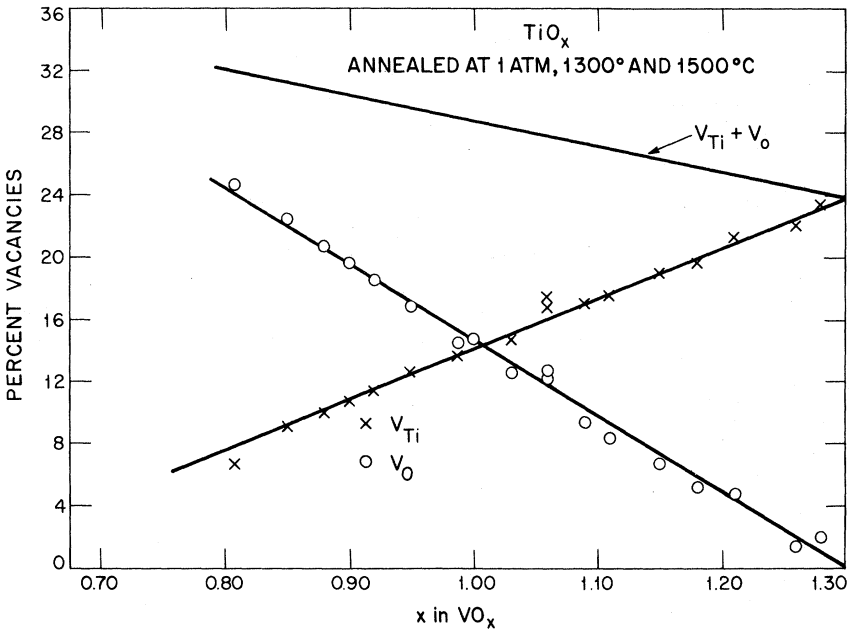

FIG. 2. Metal and oxygen vacancy concentration in TiO_x as a function of x. Solid lines are least-squares fit to data.

tected down to the limit of sensitivity of the vibrating-sample magnetometer, about 150×10^{-6} emu/mole. Ehrlich[7] reported a susceptibility at 90 K of about 75 emu/mole.

According to recent superconductivity measurements[8] on the atmospheric-pressure annealed samples used in this study, T_c for all samples lies between 0.5 and 0.9 K with rather broad transition as shown in Fig. 6. In previous experiments Hulm *et al.*[9] observed superconducting transitions for

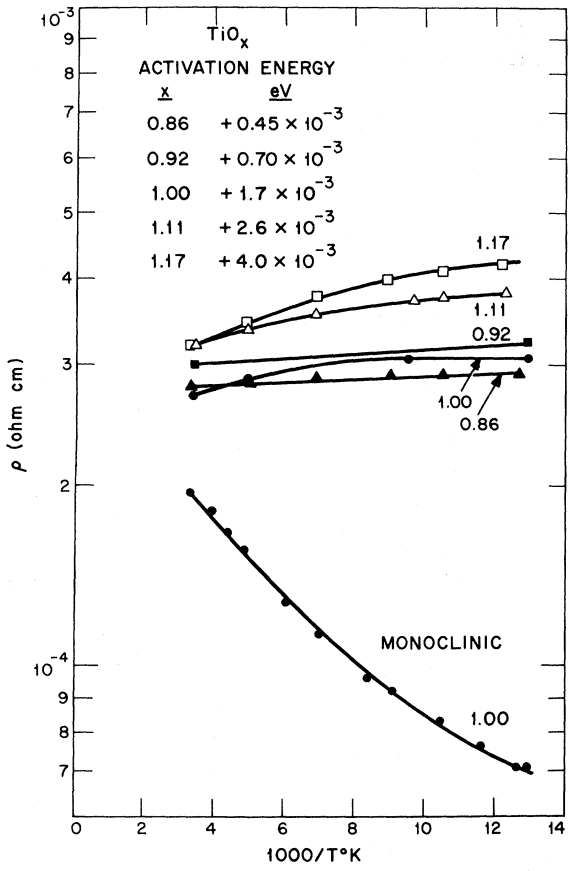

FIG. 3. Resistivity vs $1/T$ for TiO_x.

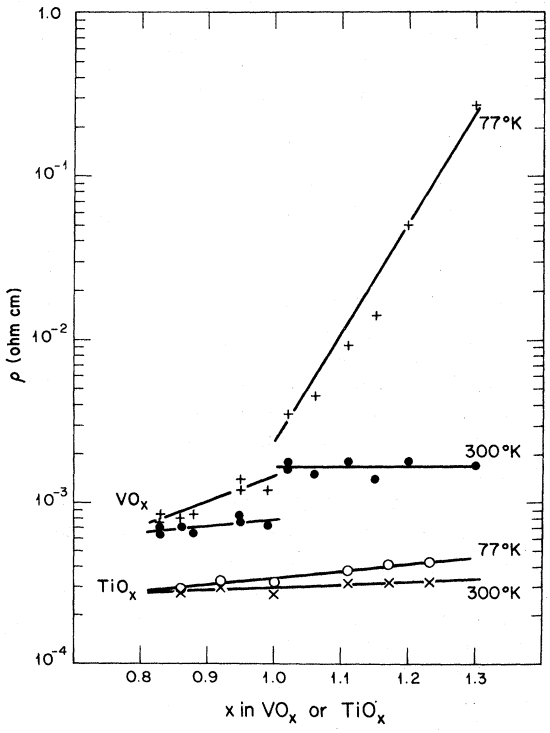

FIG. 4. Resistivity vs composition at 77 and 300 K for TiO_x and VO_x.

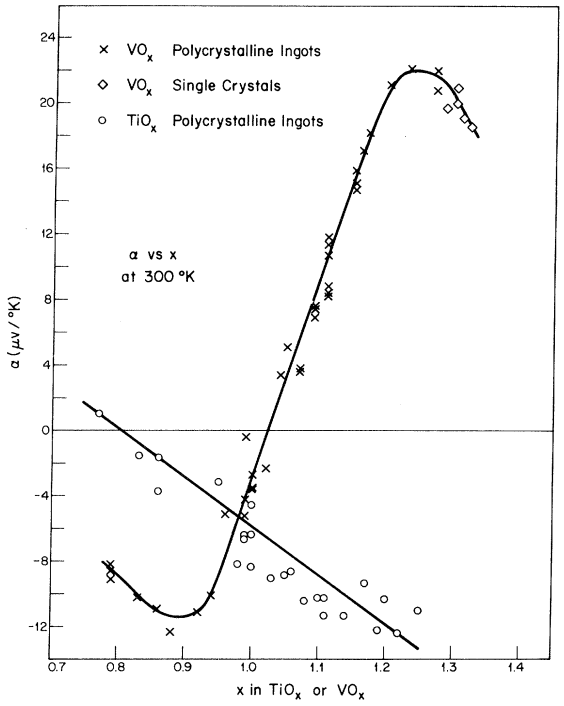

FIG. 5. Absolute Seebeck coefficient α vs x for TiO_x and VO_x.

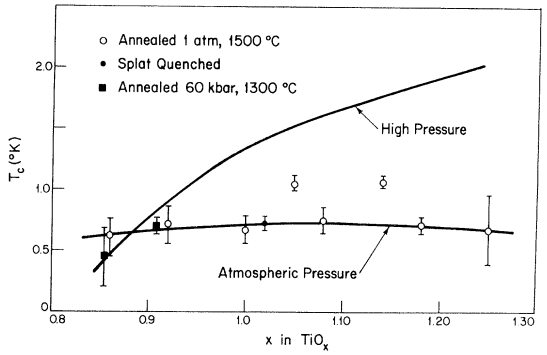

FIG. 6. Superconducting transition temperature T_c of TiO_x as a function of x. The high-pressure curve is based on the results of Ref. 10, together with the two new data points represented by squares.

$0.91 < x < 1.15$ but outside this range did not observe transitions down to 0.08 K. They commented that this was somewhat puzzling as x-ray data could pick up no evidence of a departure from the NaCl structure.

B. Cubic TiO Annealed at High Pressure

The initial motivation for the high-pressure study on TiO and VO was to determine the effect of pressure on the vacancy structure and electrical properties of these compounds. One of us found[10] that up to about 20% of the vacancies in TiO and up to 13% of the vacancies in VO could be removed by annealing samples at pressures up to 60 kbar and temperatures up to 1300 °C. Doyle *et al.*[11] report removing 100% of the vacancies in $TiO_{1.0}$ by an-

TABLE I. Effect of pressure on properties of TiO_x.

x[a]	Treatment[b]	Density (g/cm³) 1 atm	Density (g/cm³) pressed	a_0(Å) 1 atm	a_0(Å) pressed	% vacancies ($V_{Ti}+V_O$) 1 atm	% vacancies ($V_{Ti}+V_O$) pressed	Decrease in vacancies (%)	T_c of pressed (K)
0.86	D	5.057	5.117	4.189	4.205	31.5	27.2	14	0.47
0.89	A	5.043	5.162	4.191	4.200	30.5	25.0	18	<1.3
0.90	D	5.029	5.129	4.190	4.207	30.2	24.8	18	0.70
0.91	D	5.025	5.083	4.186	4.203	29.9	25.7	12	<1.25
0.95	B	5.054	5.177	4.185	4.200	27.8	21.7	22	1.6
1.00	B	5.000	5.058	4.184	4.200	28.0	23.2	17	1.35
1.01	D	4.984	5.043	4.181	4.196	29.4	24.0	18	1.45
1.03[c]	D	4.929	5.064	4.173	4.200	28.0	24.5	15	1.4
1.06[c]	C	4.975	4.996	4.174	4.196	27.1	23.3	14	1.65
1.07[c]	D	4.975	5.032	4.174	4.193	27.1	22.4	17	1.65
1.10	D	4.947	5.013	4.178	4.192	26.3	21.7	17	1.80
1.12	D	4.947	5.000	4.176	4.190	25.7	21.7	16	1.85
1.13	D	4.921	4.969	4.173	4.189	26.0	22.4	14	1.75
1.17	D	4.914	4.963	4.174	4.188	25.6	21.2	17	1.7
1.18	D	4.907	4.934	4.173	4.187	24.7	21.9	11	1.7
1.22	D	4.851	4.942	4.171	4.182	25.8	20.8	19	2.07
1.24	B	4.870	4.938	4.170	4.198	23.3	18.1	22	2.0

[a]Analysis of pressed sample ± 0.005.

[b]A, anneal at 50 kbar and 1100 °C, 2 h. B, anneal at 50 kbar and 1300 °C, 2 h. C, anneal at 60 kbar and 1100 °C, 2 h. D, anneal at 60 kbar and 1300 °C, 2 h.

[c]Duplicate samples, results identical.

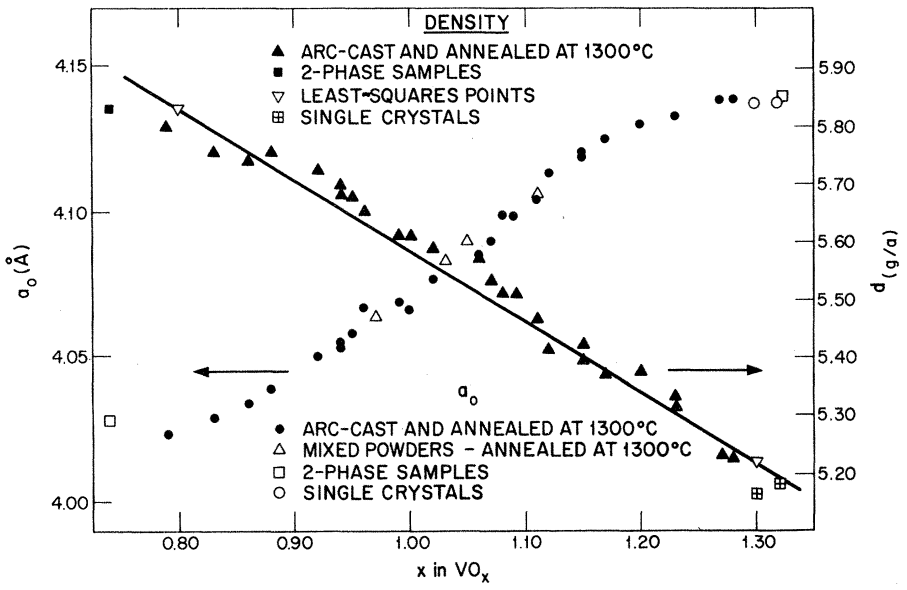

FIG. 7. Lattice parameter a_0 and measured density d of VO_x as a function of x.

nealing at 77 kbar, and 1550 °C. The lattice parameters and electrical properties of their annealed samples are similar to those reported in Ref. 10, but several of their samples have much higher density. Our results for pressure-annealed TiO are shown in Table I. It can be seen that removal of vacancies increases the lattice parameter, density, and superconducting transition temperature. Apparently TiO has become more metallic with the decrease of vacancies in spite of an attendant increase of lattice parameter.

C. Cubic VO

The lattice parameters and densities of the VO samples studied are shown in Fig. 7, and their vacancy concentrations are shown in Fig. 8. Although the dependence of vacancy concentration on x is similar to that of TiO, the lattice parameter

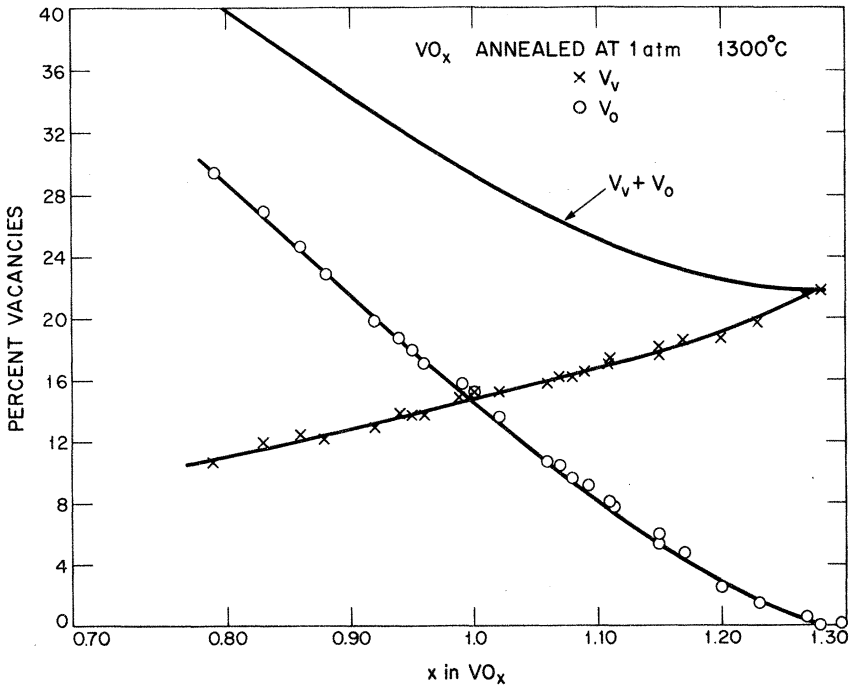

FIG. 8. Metal and oxygen vacancy concentration in VO_x.

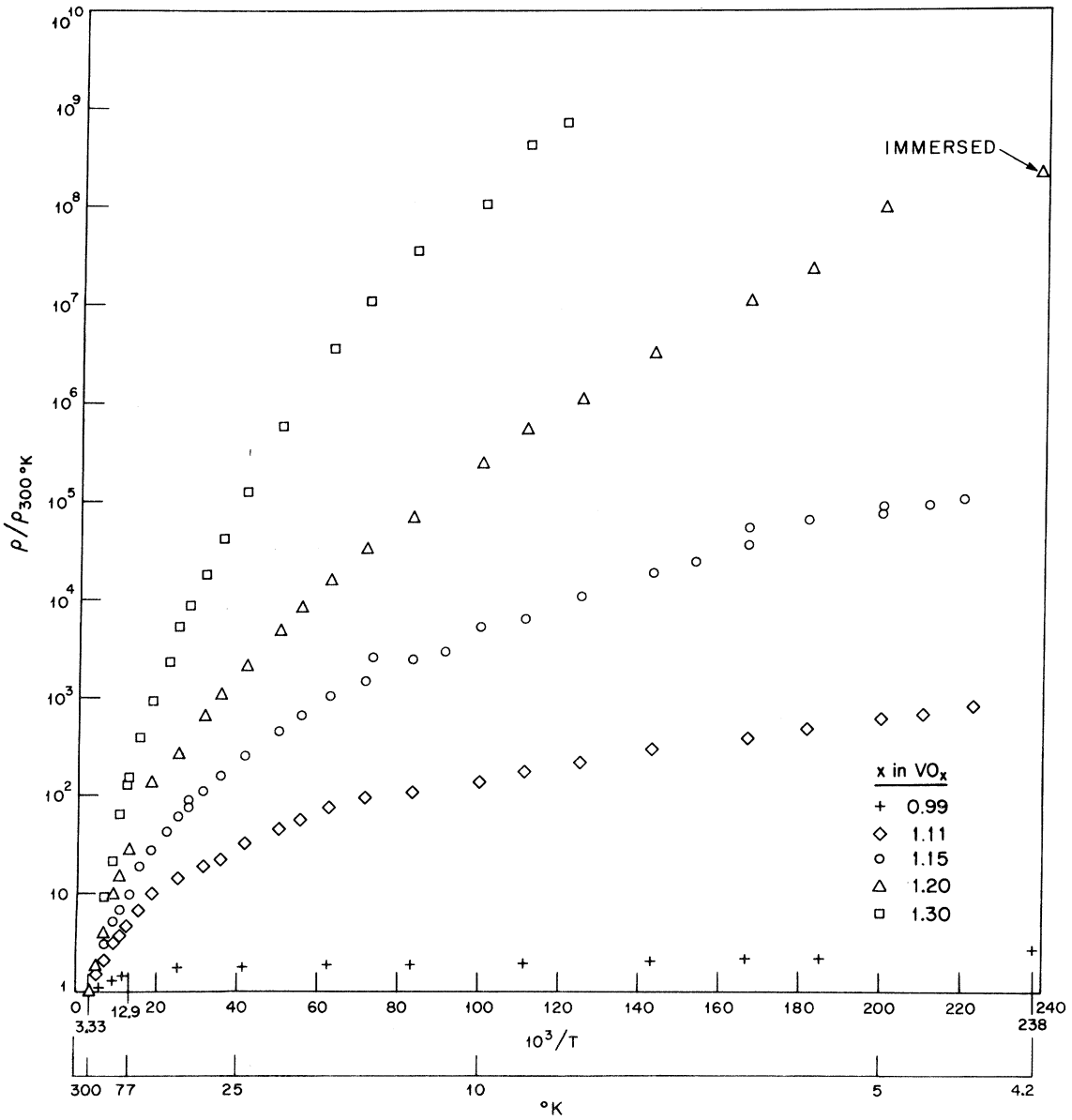

FIG. 9. Resistivity vs $1/T$ to 4.2 K for VO_x.

of VO increases with increasing oxygen content, whereas that of TiO decreases.

We find that for $x > 1.0$, the temperature dependence of ρ is qualitatively different from that for $x < 1.0$. The resistivity ρ of VO is shown as a function of x and $1/T$ in Figs. 4 and 9, respectively. Figure 10 shows the composition dependence of the activation energies calculated from the $\log_{10}\rho$-vs-$1/T$ plots of Fig. 9 in the temperature interval $150 < T < 300$ K. However, it is evident in Fig. 9 that $\log_{10}\rho$ does not vary linearly with $1/T$. In order to test the dependence of resistivity on temperature, it was assumed that $\log_{10}\rho$ was proportional to T^n, and n for each composition was determined by least-squares fit to the data in Fig. 9. It was found that the magnitude of n increases regularly from -0.075 for $x = 0.99$ to -0.56 for $x = 1.30$.

Honig *et al.*[12] have measured the resistivity, magnetoresistance, and Hall effect in some of the VO samples used in this study. They find similar values for resistivity and a negative magnetoresistance $(\rho - \rho_0)/\rho_0$ between -0.4 and -2.2 at 4.2 K in a field of 150 kG. The measured Hall coefficient is very small, $|R| < 8.6\times10^{-4}$ cm^3/C under all conditions examined, a value near the limit of

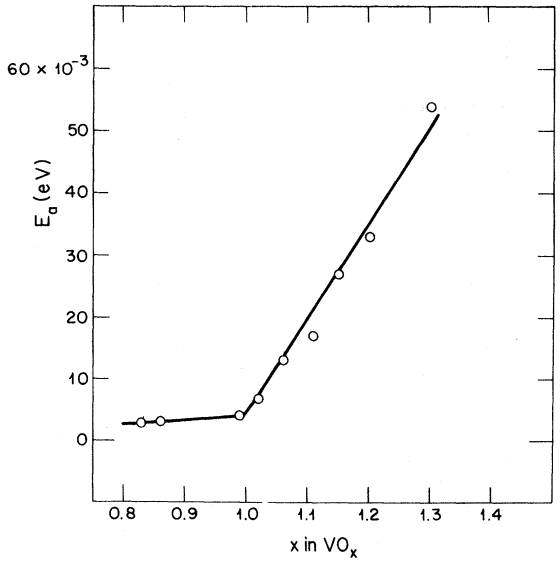

FIG. 10. Activation energy E_a vs x for VO_x calculated for $150 < T < 300$ K.

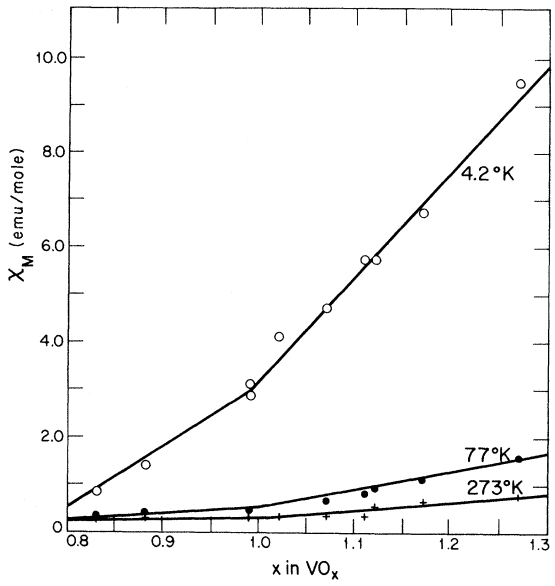

FIG. 12. Molar magnetic susceptibility χ vs x at 4.2, 77, and 273 K at 9.84 kOe for VO_x.

detection.

The Seebeck coefficient for VO_x at room temperature is shown as a function of x in Fig. 5. At $x \approx 1.0$, the Seebeck coefficient changes from negative to positive. The temperature coefficient of the Seebeck coefficient also changes sign at $x = 1.0$, as shown in Fig. 11.

The molar susceptibility for VO was measured

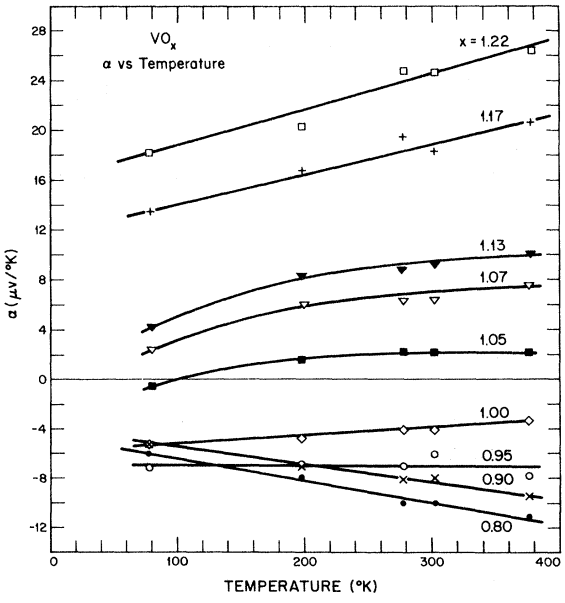

FIG. 11. Seebeck coefficient vs T for several compositions of VO_x.

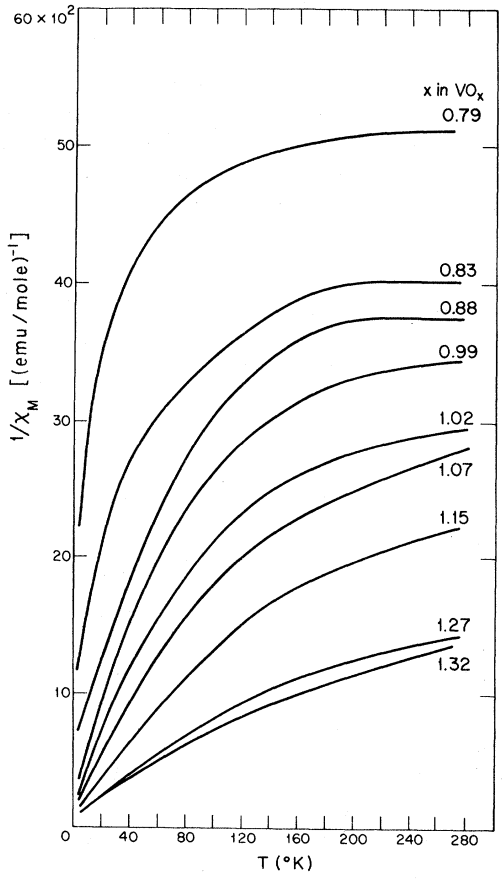

FIG. 13. $1/\chi_M$ vs T for VO_x.

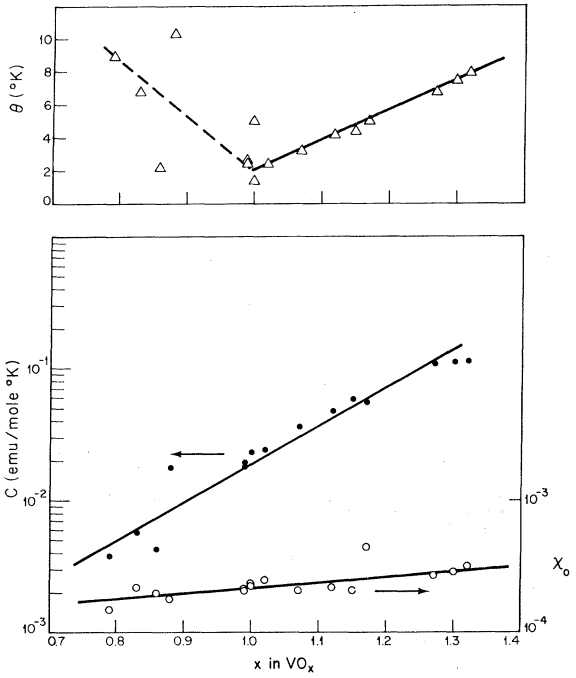

FIG. 14. χ_0, C, and θ vs x for VO_x as a function of x, where $\chi_M = \chi_0 + C/(T+\theta)$.

at 9.84 kOe as a function of temperature from 4.2 to 273 K by using a vibrating-sample magnetometer. The values of χ_M at 4.2, 77, and 273 K are plotted as a function of x in Fig. 12. At these temperatures χ_M was also measured as a function of field to 17.3 kOe.

The reciprocal susceptibility is plotted against temperature in Fig. 13. The data do not obey a simple Curie-Weiss law. However, the results can be represented as the sum of a temperature-independent susceptibility χ_0 and a Curie-Weiss term:

$$\chi_M = \chi_0 + C/(T+\theta) \quad . \tag{3}$$

The behavior of χ_0, θ, and C are shown as a function of x in Fig. 14. The temperature-independent susceptibility χ_0 is relatively constant, the Curie constant C increases exponentially with x, and the Weiss constant θ increases linearly with x for $x > 1.0$; and where $x < 1.0$, the values of θ appear to vary less consistently, but everywhere $\theta < 10$ K.

D. Cubic VO Annealed at High Pressure

Data for samples of VO_x annealed at 1100–1300 °C and pressures up to 60 kbar are given in Table II. Although the total vacancy content is reduced by as much as 13%, the electrical properties are remarkedly unaffected.

IV. DISCUSSION

This work was undertaken to provide an extensive body of coherent experimental data on the systems TiO_x and VO_x. The variation with x of a number of properties of both compounds is summarized in Fig. 15. Table II lists the properties of the stoichiometric compositions $TiO_{1.00}$ and $VO_{1.00}$, and also the properties recently measured in the laboratory[13] on single crystals of the closely related

TABLE II. Properties of $TiO_{1.00}$, $VO_{1.00}$, and $NbO_{1.00}$ at 300 K unless otherwise noted.

Property	$TiO_{1.00}$	$VO_{1.00}$	$NbO_{1.00}$
Structure	NaCl cubic with 15% random vacancies	NaCl cubic with 15% random vacancies	NaCl cubic with 25% ordered vacancies, or simple cubic with no vacancies
Lattice parameter (Å)	4.184	4.071	4.211
Density (g/cm^3)	5.00	5.60	7.24
Color	gold	silver	silver
Melting point (°C)	incongruent	incongruent	1945
Resistivity (Ω cm)			
300 K	310×10^{-6}	720×10^{-6}	20×10^{-6}
4.2 K	...	1900×10^{-6}	0.7×10^{-6}
Thermoelectric power (μV/K) 300 K	−6.0	$<\pm1$	$<\pm1$
Magnetic susceptibility at 4.2 K (emu/mole)	80×10^{-6}	300×10^{-6}	116×10^{-6}
Superconducting transition temperature (K)	0.7	Not detected down to 0.3 K	1.45

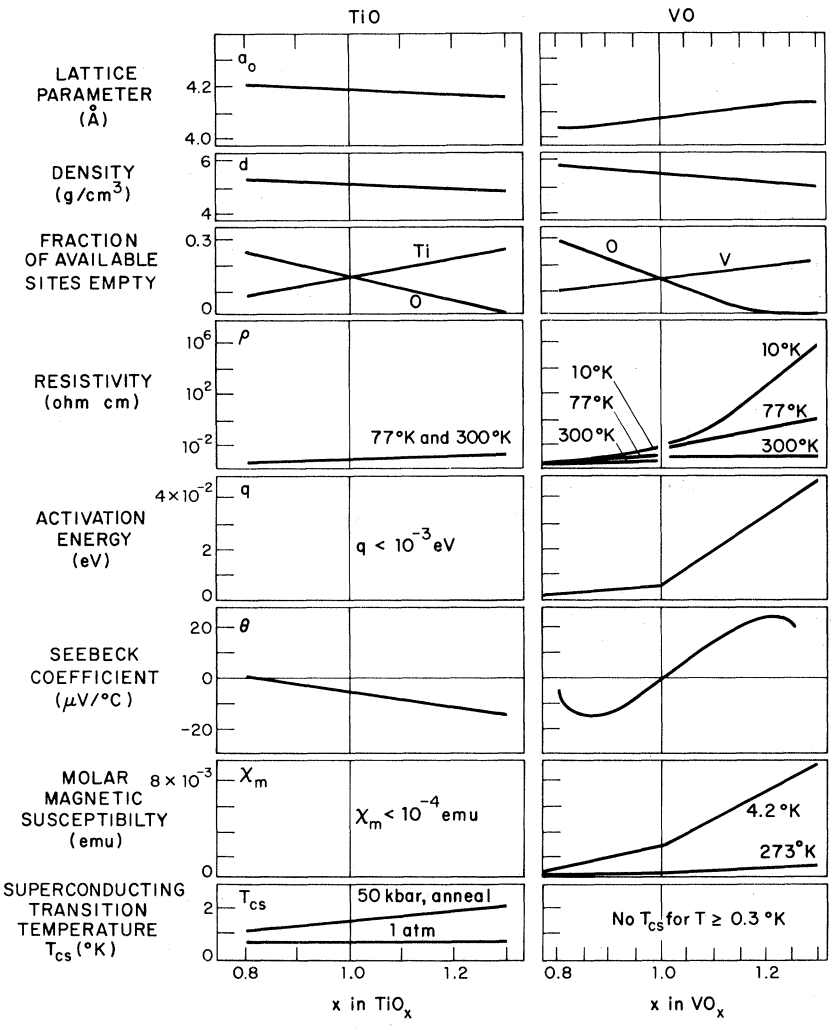

FIG. 15. Summary of properties of TiO_x and VO_x.

compound $NbO_{1.00}$.

Rather than suggesting explanations for a few aspects of these data, we content ourselves with raising several of the most striking questions concerning the data that any comprehensive theory will have to answer. Why are such high percentages of vacancies stable in these two compounds, a behavior found elsewhere only in NbO, which has 25% vacancies in the face centered cubic lattice (or no vacancies in its own simple cubic lattice)? Why are the resistivities of TiO_x for all x and of VO_x for $x<1$ so constant at all temperatures, while for $x>1$ the resistivity of VO_x becomes quite temperature dependent? Why does the Seebeck coefficient change sign for VO_x at $x=1.0$? Why is TiO_x a superconductor for all x, while VO_x is not superconducting above 0.3 K for any x? The companion theoretical paper by Goodenough[14] addresses itself to these and other questions.

ACKNOWLEDGMENTS

The authors are grateful to J. B. Goodenough for many helpful suggestions from the initiation of this study to its completion. We also express our gratitude to E. B. Owens for chemical analysis and Miss M. C. Finn and Mrs. M. J. Button for electron-probe measurements and determination of lattice parameters.

---

†Work was sponsored by the Department of the Air Force.

*Present address: Boston University Marine Program Marine Biology Laboratory, Woods Hole, Mass. 02543.

[1]M. D. Banus and T. B. Reed, in *The Chemistry of Extended Defects in Non-Metallic Solids*, edited by M. O'Keeffe (North-Holland, Amsterdam, 1970), p. 488. Some of the data appearing here were presented in this reference, but particular measurements have been extended to other compositions or temperatures to make a

more coherent study. Details of experimental technique are also described in this reference.

[2]T. B. Reed, in *High Temperature Technology*, edited by N. K. Hiester (Butterworths, London, 1969), p. 655.

[3]L. J. van der Pauw, Philips Res. Rept. 13, 1 (1958).

[4]D. Watanabe, J. R. Castles, A. Jostens, and A. S. Malin, Acta Cryst. 23, 307 (1967).

[5]S. P. Denker, J. Appl. Phys. 37, 142 (1966).

[6]S. Takeuchi and K. Suzuki, J. Japan Inst. Metals (Sendai) 33, 279 (1969); 33, 284 (1969).

[7]P. Ehrlich, Z. Electrochem. 45, 362 (1939).

[8]M. D. Banus, T. B. Reed, M. Sjöstrand, and P. Keesom (unpublished).

[9]J. K. Hulm, C. K. Jones, R. Mazelsky, R. C. Miller, R. A. Hein, and J. W. Gibson, in *Low Temperature Physics*, edited by J. G. Daunt (Plenum, New York, 1965), p. 600.

[10]M. D. Banus, Mater. Res. Bull. 3, 723 (1968).

[11]N. J. Doyle, J. H. Hulm, C. K. Jones, R. C. Miller, and A. Taylor, Phys. Letters 26A, 604 (1968).

[12]J. M. Honig, W. E. Wahnsiedler, M. D. Banus, and T. B. Reed, J. Solid State Chem. 2, 74 (1970).

[13]E. R. Pollard, Ph. D. thesis (MIT, 1968) (unpublished).

[14]J. B. Goodenough, preceding paper, Phys. Rev. B 5, 2764 (1972).

PHYSICAL REVIEW B VOLUME 5, NUMBER 8 15 APRIL 1972

Determination of the Surface-Plasmon Dispersion Relation in Aluminum by Inelastic Electron Diffraction*

A. Bagchi
Department of Physics and Materials Research Laboratory, University of Illinois, Urbana, Illinois 61801
and The James Franck Institute, University of Chicago, Chicago, Illinois 60637

and

C. B. Duke
Department of Physics, Materials Research Laboratory and Coordinated Science Laboratory, University of Illinois, Urbana, Illinois 61801

(Received 8 December 1971)

Inelastic differential cross sections for low-energy ($10 \lesssim E \lesssim 10^3$ eV) electrons scattered from the (111) and (100) surfaces of aluminum are analyzed using a quantum field theory of inelastic processes. The analysis permits the determination of the dispersion relation and damping of excitations created by the electrons. For nominally clean Al(111), the surface-plasmon dispersion relation is found to be $\hbar\omega_s(p_\parallel) = 10.1 - 0.7p_\parallel + 10p_\parallel^2$, $10^{-2} \lesssim p_\parallel \lesssim 1$ Å^{-1}, for momenta measured in reciprocal angstroms and energies measured in electron volts. With this choice of the dispersion relation, the predictions of the theory also are in fairly good agreement with experimental inelastic scattering data from Al(100) surfaces. The accuracy of the method of analysis and possible improvements on it are discussed.

I. INTRODUCTION

Since the work of Ritchie[1] and Stern and Ferrell[2] establishing the existence of surface plasmons, their dispersion relation has interested both theorists and experimentalists. Surface plasmons are elementary excitations of a bounded electron gas. A study of their dispersion relation is useful for understanding the electronic properties of metal surfaces. For example, a knowledge of both the surface-plasmon dispersion relation and the electron–surface-plasmon coupling vertex is a necessary prerequisite to the construction of a theory[3] of the electron-metal interaction near the metal surface. The dispersion relation also may be important in a detailed theory of the processes of chemisorption and catalysis.

The surface-plasmon dispersion relation has been studied by Kanazawa[4] using an approximate quantum-mechanical theory, and by Ritchie and Marusak[5] in the hydrodynamic model. Microscopic derivations of this quantity have been given by Fedders[6] and Feibelman [7] who also studied surface-plasmon damping in the random-phase approximation (RPA). The full RPA integral equation for a surface-charge fluctuation recently has been solved[8,9] numerically to obtain the dispersion and damping of surface plasmons. Most theories predict a linear dependence of the surface-plasmon energy on its momentum $p_\parallel$ parallel to the surface, for small values of this quantity. (This result is valid in the limit that the effect of retardation, which is important for $p_\parallel \lesssim 10^{-3}$ Å^{-1}, can be ignored.) If we retain terms to second order in the momentum, then the energy and damping of surface plasmons may be written as

$$\hbar\omega_s(p_\parallel) = \hbar\omega_s + C_1 p_\parallel + C_2 p_\parallel^2 , \qquad (1)$$